International Journal of Steel Structures
https://doi.org/10.1007/s13296-021-00515-9

Online ISSN 2093-6311
Print ISSN 1598-2351

Flexural Behavior of Encased Beam Flat or Perforated steel Cold Formed Sections

Ashraf Abou-Rayan[1] · Nader Khalil[1] · Ahmed Youssef[1] · Mohamed Eldeib[1]

Received: 4 October 2019 / Accepted: 9 July 2021

Abstract
This paper presents an experimental study on the flexural behavior of encased flat cold formed steel sections FCFS and perforated cold formed steel sections PCFS. A full scale eleven specimens were prepared and tested till failure. One specimen without steel cold formed section tested as a control beam. Six specimens with flat steel cold formed section were tested to figure out the enhancement effect of section area and position. Finally, four specimens with a new shape of perforated steel cold formed sections were tested with different positions. Cold formed steel section height, flange width, and position are the main parameters studied and investigated. The ultimate load and vertical deflections were recorded and investigated. Also, modes of failure of the control and composite concrete beams were studied. From the experimental investigations, it has been observed that there is significant increase in ultimate load of composite beams with a perforated steel cold formed section. A significant increasing in the ultimate load was observed for specimens with perforated steel cold formed section

Keywords CFS section · Composite section · Perforated steel · Smooth steel · Structural behavior

1 Introduction

Thin sheet steel products are extensively used in building industry, and range from purlins to roof sheeting and floor decking. Generally these are available for use as basic building elements for assembly at site or as prefabricated frames or panels. These thin steel sections are cold-formed, i.e. their manufacturing process involves forming steel sections in a cold state from steel sheets of uniform thickness. Recently, cold formed steel sections are widely used as bottom reinforcement in composite beams to rise its load capacity. In such constructions, concrete and steel flexural behavior were studied. Kamal and Khalil (2017) have studied a series of bending tests to examine the influence of encasing cold-formed steel (U-section) in a reinforced concrete beam on the beams capacities, mode of failure and ductility. They have found that the cold-formed steel (U-section) increased the beam load carrying capacity and improved the beam ductility. It has observed that encasing the formed steel sections reduced the influence of the steel sections local buckling. Wehbe et al. (2013) had examined full-scale specimens as a series of experimental studies on representing concrete/CFS flexural beam under vertical loads. The studies were fabricated to investigate the structural behavior of concrete/CFS beams and concrete/CFS headers. They had investigated that using stand-off screws as shear connectors is feasible for providing composite action. When number and spacing of stand-off screws are provided, the CFS section acts as tension reinforcement under positive bending moment and the concrete/CFS composite beams can attain their full flexural capacity. Alhajri et al. (2016) had examined nine precast composite beam, in which the channel sections were used to act compositely with the ferro-cement slabs to investigate the number of wire mesh used in ferro-cement slab and the steel section thickness. The results showed that in full-scale CFS specimens of 4 mm thickness carried 83.7–113.9% higher ultimate bending moment than 3 mm and 2 mm CFS thickness. This was expected, because ultimate loads of members increases with a higher of CFS thickness. Tahir et al.

✉ Mohamed Eldeib
Mohamed.Thabet@bhit.bu.edu.eg

Ashraf Abou-Rayan
Ashraf.aborayan@bhit.bu.edu.eg

Nader Khalil
nader.gerges@bhit.bu.edu.eg

Ahmed Youssef
ahmed.mohamed@bhit.bu.edu.eg

[1] Department of Civil Engineering, Benha Faculty of Engineering, Benha University, Benha 13512, Egypt

Published online: 15 July 2021

(2016) had studied eight push-out test specimens of shear connector with bolts size consist of M12, M14 and M16 of grade 8.8 and were tested to failure. The experimental results explained that the bolted shear connectors used to possess good shear resistance capacity. Good agreement was realized between experimental and theoretical results of specimens with 8 number of shear connectors with a ratio between 0.97 and 1.42. Influence of changing the size of the bolted shear connectors was deducted. The results explained that the size of bolted shear connectors affected the ultimate strength capacity of the shear connectors significantly. Valsa Ipe et al. (2013) had tested specimens consisted of composite channel (with lip laied on tension side and compression side) and box sections, the behavior which was compared with companion empty sections. To understand the role of shear connectors in improving the composite action, some of the composite sections were provided with novel conventional bolt type and simple bar type shear connectors in the shear zone of beams. They had concluded that the load carrying capacities of composite channel and box sections without shear connectors were found to be 32.26% and 38.77% respectively more than empty box and channel sections. Bamaga et al. (2013) had said that the use of composite beam consisting of cold-formed steel close box and filled with concrete or open could also reduce construction cost. They had deducted that the use of CFS section as replacement for the conventional reinforcement bars in conventional reinforced concrete beams, composite-filled concrete beams, composite bridge girders and conventional composite beams. The adequate strength capacity could be achieved by using CFS sections in conventional composite beam. However, the ductility requirement is still insufficient. Thus, future studies focused on this issue are recommended. Ye et al. (2018) had studied 36 axial compression tests on CFS channel specimens with different lengths (1 m, 1.5 m and 2 m) and different four cross-sections under a concentrated applied load and boundary conditions. They had concluded that Additional overall bending moment of the specimens, coming from a moving of the effective centroid, was observed after the appearance of a local buckling pattern. Bending consistently occurred towards the web in the plain channels and towards the lips in the lipped channels. Hsu et al. (2014) had studied six specimens with 12 ft long composite beams indicate that the suggested composite beam system presents the better performance of structural ability for both ultimate strength and ductility of the composite section. The ultimate strength and ductility of suggested composite section can be increased by 14–38% and 56–80%, respectively, as compared to an empty section or built-up section in all tests. The longitudinal shear crack of concrete slab can be prevented by providing transverse shear reinforcement in the concrete slab. Kvočák et al. (2013) had presented an experimentally validated composite steel and concrete beams using a modified form of the closed section steel with static load tests. They had investigated that a Plate bridges with composite beams are suitable for constructing bridges of a short and medium range. The individual load cases represent an additional load or lightweight of the samples during the experimental tests. When unloading, a permanent deflection was recorded which, was due to changes in bending stiffness after cracking in concrete.

Paolo Foraboschi (2016) was entrusted with the task of redesigning the floor, which had to constitute the stories of a further nine buildings of the construction lot, whose floors had been designed equal to the floor that had failed, and neither the spans nor the thickness could be changed. The new floor was built using a different construction method as well. The load was left on the floor for 3 years and the deflections increased only moderately. Paolo Foraboschi (2019) had studied the interaction of flexure and compression in steel beam-columns with fixed roller boundary conditions. It was shown that, for those end restraints, the effective length factor approach is inaccurate to account for geometric nonlinearity. A detailed account of the formulation and some examples that showed differences from the results obtained from conventional and code formulas was provided. Paolo Foraboschi (2020) delivered a plain analytical formulation for predicting the ultimate combinations of axial force and bending moment, allowing for material and geometric non-linearities. The formulation easily permits the ultimate interaction diagram of a steel member to be accurately constructed, as well as the structure to be checked for combined axial force and lateral load. It were applied specifically to columns but can be used for any members. Faridmehr et al. (2016) had presented an experimental, analytical and numerical deduction on the correlation between non-dimensional slenderness and pure bending strength of stiffened cold-formed steel as a construction material. Cover plates with different thicknesses of (1.6, 2 and 4 mm) were presented to evaluate the slenderness effects on flexural performance of CFS-sections laied at top flanges only as it would be the predicted location for local and distortional buckling to investigate the bending moment capacity and buckling modes of specimens with different cover plate thicknesses. They had concluded that the design strengths predicted by the current Direct Strength Method in accordance with the American specification guideline, AISI, was conservative for study sections as these sections can improve plastic moment. Utilizing cover plates at top flange in cold-formed C-channel sections would reduce non-dimensional slenderness that would eventually improve buckling capacities**. Dinis and Camotim (2010) had concluded that the flange local buckling and the distortional buckling are the main factors governing the failure modes of the steel cold-formed sections (CFS), arising from in-plane bending moments. J. Lee et al. (2005) had optimized the (CFS) elements by reducing the dimensions of the cross sections, while W.Ma et al.

(2015) had optimized the (CFS) elements by using Genetic Algorithms according to EC3. J.Z. Leng et al. (2014) have optimized the (CFS) elements by incorporating some end-user constraints and have limited the manufacturing process to a certain numbers of rolling. Our research presents an experimental investigations to assess the flexural behavior of encased flat and perforated cold formed steel sections. A full scale eleven specimens were examined to failure. The ultimate load and vertical deflections were registered and investigated. Also, modes of failure of the concrete/CFS beams were studied. Cold formed steel section depth, flange width, and positions were the main parameters studied and investigated. New shape of perforated cold formed steel sections is presented in the paper. Also, exploring the best enhancement of the concrete/CFS beam.

2 Experimental Work

Eleven simply supported composite beams having the same rectangular concrete section (200*400) mm with total length of 3050 mm and clear span of 2850 mm were tested to explore the structural behavior of the encased flat and perforated steel cold formed sections. Specimens were loaded by mid span concentrated load. All specimens were reinforced longitudinally with two bars with a diameter of 12 mm top and bottom, the steel grade used was 360/520. The specimens were also reinforced transversely by 6 stirrups with 8 mm diameter per meter, with steel grade of 240/360. One of the tested specimens was tested as a control beam without CFS section. Four specimens have PCFS with full compression flange width and varied depths were embedded in the concrete section in two positions (back to back and face to face). Also, two specimens have PCFS with half compression flange width and varied depths width in one position (back to back). Finally, four specimens have perforated CFS embedded in concrete as back to back, face to face, u-shape, and n-shape. The dimensions of the concrete beam and its longitudinal and transverse reinforcements were shown in Fig. 1. The perforated steel cold formed sections details and dimensions were shown in Fig. 2. Finally, the experimental program and cross sections details were summarized in Table 1 and shown in Fig. 3.

A0 indicates the control beam without CFS sections. The first letter (B, C) indicates the group of flat CFS sections. The first letters (DS, ES) indicates the group of perforated CFS sections. The second letter (F, T) indicates the CFS section height Full depth, and Third depth. The third letter (F, H) indicates the CFS section top flange width Full, and Half width. The numbers (1, 2) in groups (A, B, C, D) indicates the CFS position back to back, and front to front. The numbers (1, 2) in group (E) indicates the CFS position u-shape, and n-shape.

There are two systems that connects steel to concrete:

1. The flat cold formed steel sections were impeded in concrete without shear connectors and covered by stirrups, upper, and lower long steel.
2. The stirrups traverse through the holes of the perforated cold formed steel sections and act as a shear connectors as shown in Fig. 2.

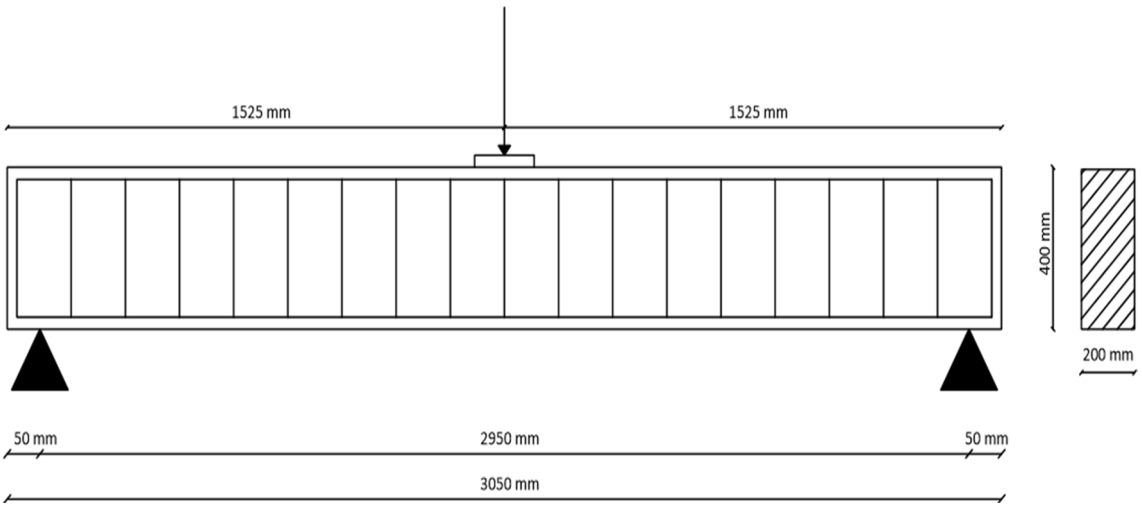

Fig. 1 Typical dimensions of specimens without steel sections

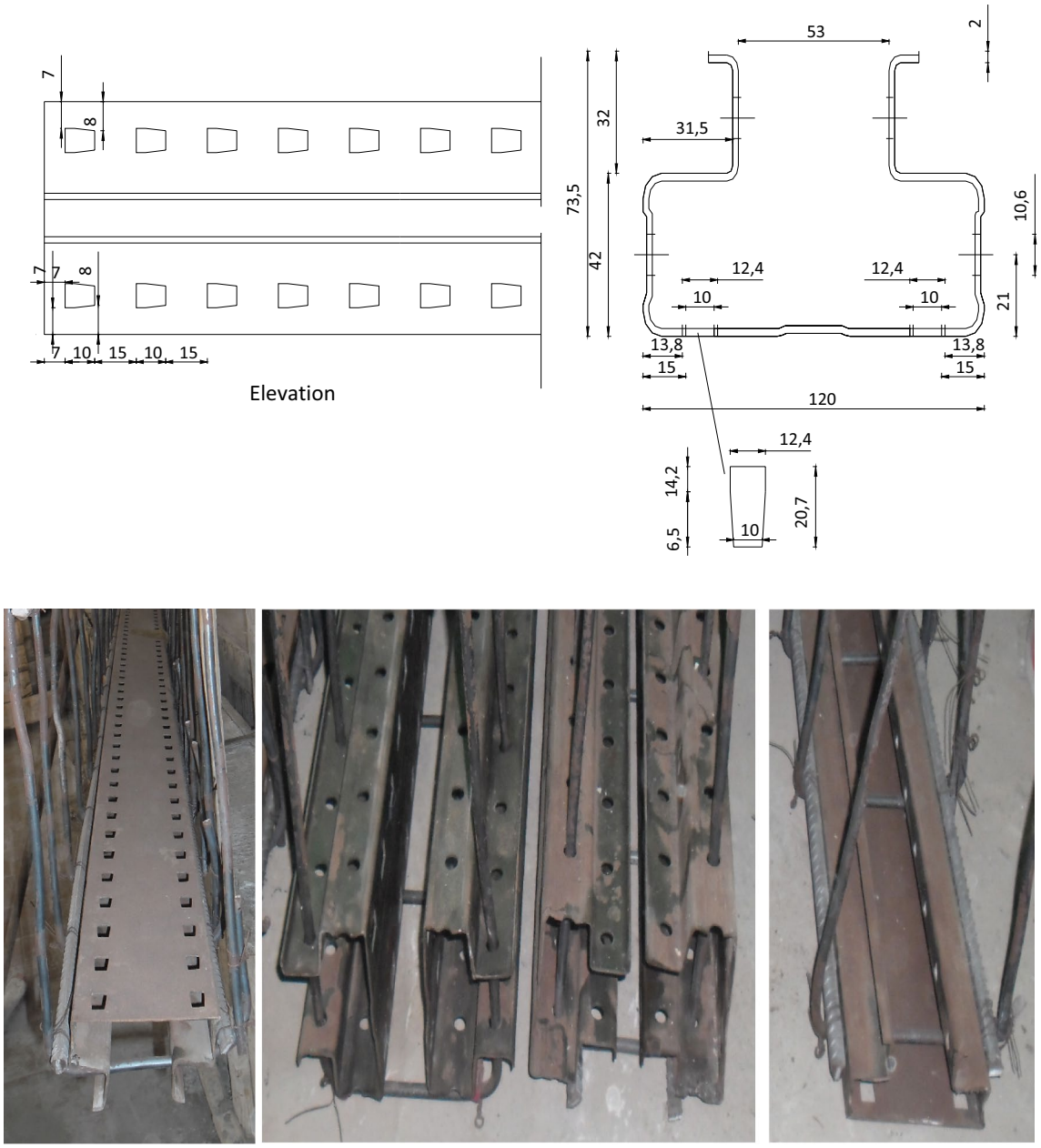

Fig. 2 Typical detail of steel perforated cold formed section

3 Material Properties

3.1 Concrete

Concrete composed of ordinary Portland cement, siliceous sand and a crushed stone course as an aggregate of 10 mm maximum size. Trial mixes were used to determine a suitable mix design. The properties of concrete specimens were determine from nine cubes. A recommended concrete mixture were composed of 400 kg of Portland cement to 0.60 cubic meter of sand to 0.6 cubic meter of crushed stone. Development of concrete strength was observed closely by testing the cubes after 7 and 28 days. The average value of compressive strength obtained from cube tests is $f\mathrm{cu} = 31.03\ \mathrm{N/mm^2}$. Splitting tensile strength form cylinders tests is $f\mathrm{t} = 3.3$ N/mm2. Slump test was carried out on fresh concrete to check the workability and consistency of concrete. The slump test results were acceptable according to the Eurocode code, as shown in Fig. 4.

Table 1 Experimental program

Series	Specimens	Steel cold formed sections details					
		Qty	Depth (mm)	Comp. F width (mm)	Thick. (mm)	Section position	Area (mm^2)
A	A0	No CFS section					
B	BFF1	2	305	62	1.5	B. to B	1287
	BFF2	2	305	62	1.5	F. to F	1287
	BFH1	2	305	31	1.5	B. to B	1194
C	CTF1	2	120	62	2.4	B. to B	1171.2
	CTF2	2	120	62	2.4	F. to F	1171.2
	CTH1	2	120	31	2.4	B. to B	1022.4
D	DSTF1	2	120	73.5	2.0	B. to B	1108
	DSTF2	2	120	73.5	2.0	F. to F	1108
E	ESFH1	1	120	73.5	2.0	Horizontal	554
	ESFH2	1	120	73.5	2.0	H. Inverted	554

3.2 Steel Sections

The tensile properties of the steel cold formed sections were determined in accordance with ASTM procedure ASTM-A370-ASME-SA-370. This specimen is used for testing metallic materials in the form of sheet strip in nominal thickness from 0.005 to 1 in. (0.13 to 25 mm). Three coupons were tested to failure. The Mechanical properties are given in Table 2.

4 Test Setup

The control concrete beam and the encased CFS composite beams were tested as simply supported to failure. The load was applied the middle span of the specimen by using a hydraulic jack of 400 kN capacity were used in concrete laboratory at Benha faculty of engineering Benha University. Deflections were measured using Linear Variable Deformation Transducers (LVDTs) located under the concrete sections at four points through beam length L/2, L/4, L/6 and L/3. All load cell and LVDTs were connected to a data acquisition system which was programmed to record the output data, as shown in Fig. 5. During loading, the readings were observed and automatically recorded. The specimen was loaded every 70 KN more or less until failure load. Cracks were observed and recorded at its corresponding load. The ultimate load and the failure mode for specimens were recorded and concrete cracking was marked.

5 Results and Discussion

Loads and vertical deflections of the tested specimens were recorded up to failure. The deflected shape of the tested specimens at the first crack loads and the ultimate loads due to the LVDTs record were shown in Fig. 6. Ultimate loads, first crack loads and the corresponding vertical deflections were listed in Table 3. Also, the modes of failure of each specimens were observed and listed.

5.1 Modes of Failure

Three types of cracks were observed. The first mode occurred due to flexure mode at the bottom side of the specimen, especially at mid span for specimens (A0, BFF1, BFH1, CTF1, CTH1, DSTF1, ESFH1, and ESFH2). The second type occurred due to the stress concentration on the bottom steel flange due to shear splitting (Concrete which causes a longitudinal splitting cracks of concrete at the flange line) for specimens (CTF1, and CTH1). The third type of failure was lateral torsional buckling for specimens (BFF2, CTF2, and DSTF2). For all tested specimens, all cracking types were observed and the second type was occurred suddenly after the first type was observed, as show in Fig. 7.

5.2 Effect of Using CFS in Concrete Beam

Increasing beam ultimate load and stiffness were expected previously by using steel cold formed sections in concrete beam. Loads and vertical deflections at mid span relationships of the tested groups compared with control beam results are shown in Fig. 8. As shown in Fig. 8a, full depth CFS with different configurations (group B) enhance the control beam ultimate load by 96.72%, 75.41% and 113.11% for BFF1, BFF2 and BFH1 respectively. Also, using CFS with half depth (group C) increase the control beam ultimate load by 125%, 59.85% and 125.14% for CTF1, CTF2 and CTH1 respectively as clarified in Fig. (8b). New shape of the perforated steel cold formed sections indicates a good enhancement of the control

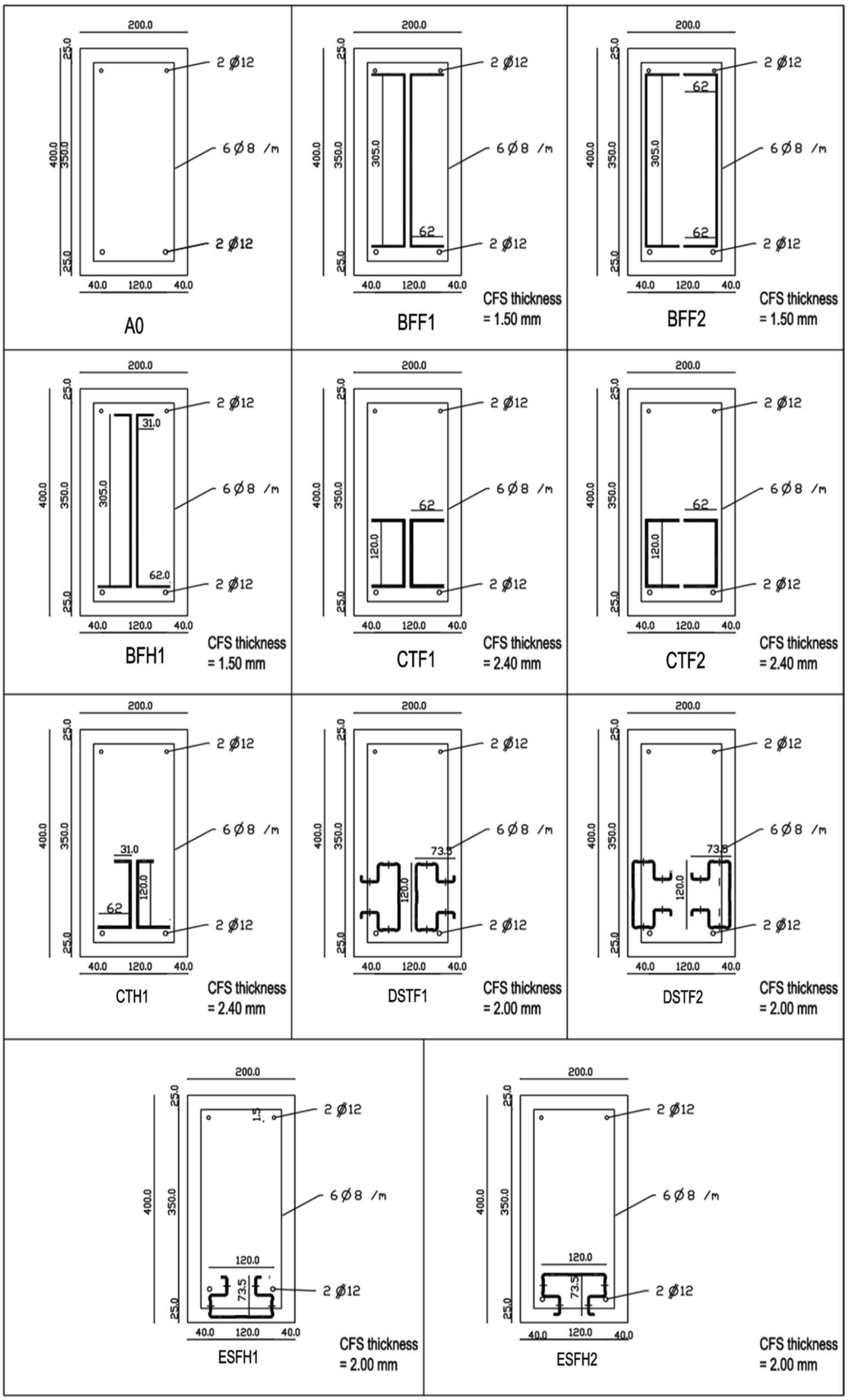

Fig. 3 typical sections of the tested specimens (all dimensions in mm)

Fig. 4 Laboratory concrete test

Table 2 Mechanical properties of steel plates

Modulus of elasticity (N/mm^2)	Yield stress (N/mm^2)	Ultimate strength (N/mm^2)	Yield strain (εy) %	Strain at ultimate strength (εu)%
208,900	246	365	0.50	3.5

beam ultimate load as shown in Fig. (8c, d). Group D, the ultimate load of composite beam with perforated CFS increased by 158.19% and 107.65% for DSTF1 and DSTF2 respectively compared with ultimate load of the control beam. Finally, (group E) composite beam with single horizontal perforated CFS figure out a considerable raising of the control beam ultimate load by 103.55% and 103.41% for ESFH1 and ESFH2 respectively.

5.3 Effect of CFS Position

Steel cold formed section positions show direct and significant enhancement on the flexural behavior of the CFS composite beam. Back to back and face to face positions are studied and investigated here for full depth, half depth and perforated CFS. It can be observed that for full depth CFS back to back increase ultimate load by 12.15% of that obtained for the face to face position. This increasing percentage are reached to 40.76% for half depth CFS. Finally, for perforated CFS, back to back position increase the ultimate load by 24.43% than face to face position. So, it can be concluded that encasing CFS by concrete in the position of back to back is more significant than face to face one. Figure 9 clarify the effect of CFS positions on the flexural behavior of the composite beam in case of full depth (group B), half depth (group C) and perforated (group D).

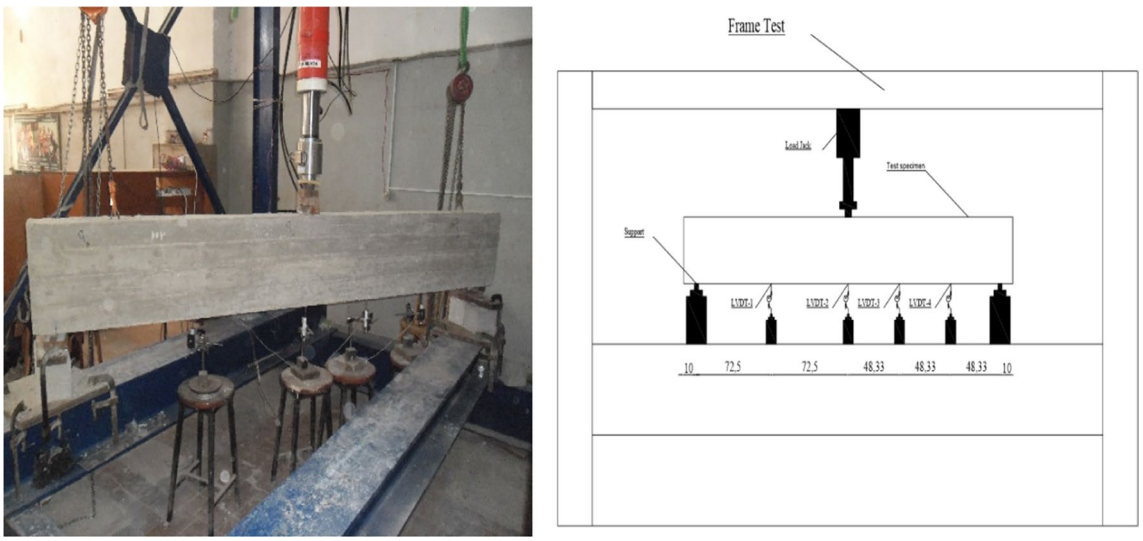

Fig. 5 Test setup

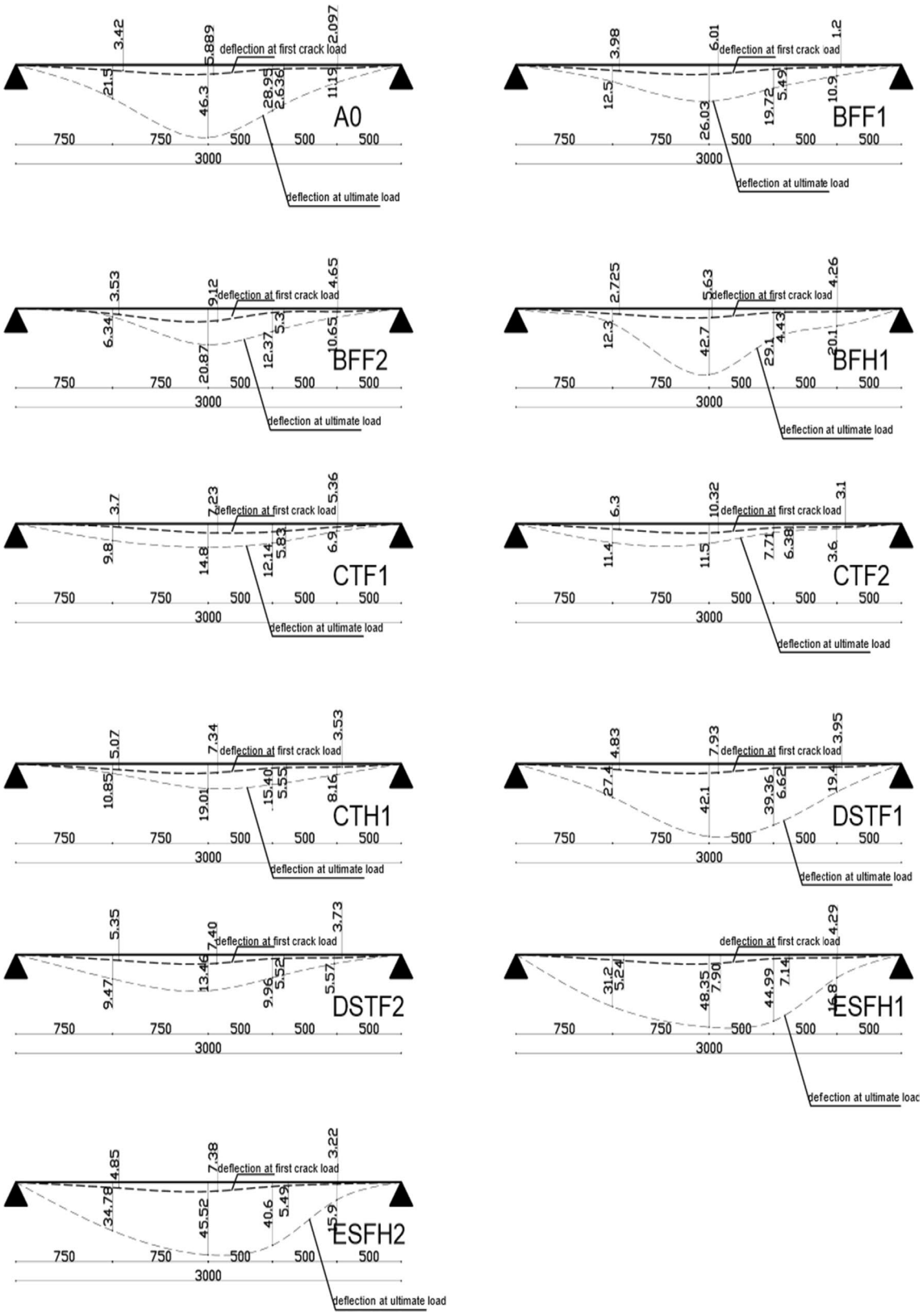

Fig. 6 The deflected shape of the tested specimens at first crack and ultimate loads

Table 3 Specimens test results

Series	Specimens	First crack		failure		Modes of failure
		Load (kN)	Deflection at mid span (mm)	Load (kN)	Deflection at mid span (mm)	
A	A0	40	5.89	73.2	46.3	Flexural failure
B	BFF1	85	6	144	26.03	Flexural failure
	BFF2	100	9.12	128.4	12.36	Flexural and shear splitting
	BFH1	83	7.43	156.5	42.74	Flexural failure
C	CTF1	113	7.23	164.7	14.78	Flexural and shear splitting
	CTF2	110	10.32	117	11.47	Failure at bearing
	CTH1	104	7.34	164.8	19.01	Flexural failure
D	DSTF1	117	7.93	189	42.10	Flexural failure
	DSTF2	100	7.40	152	13.46	Flexural and shear splitting
E	ESFH1	104	7.90	149	44.99	Flexural failure
	ESFH2	95	7.38	148.9	40.61	Flexural failure

5.4 Effect of CFS Top Flange Width

Decreasing top flange width increase significantly the ultimate load of full depth CFS. But, has no effect in case of half depth CFS. Loads and vertical deflections relationships of the reduced top flange compared with full flange are shown in Fig. 10a, b for full and half depth CFS. It was observed that reducing top flange width led to increase the ultimate load by 8.7% and 0.1% for full and half depth CFS respectively.

5.5 Effect of CFS Depth

Using the same CFS area with different depths affect the flexure behavior of the composite beam. To figure out the effect of CFS depth, group B specimens were compared with its corresponding specimens in group C. Figure 11a–c present loads and vertical deflections relationships for (BFF1 & CTF1), (BFF2 & CTF2) and (BFH1 & CTH1). It was observed that, for back to back position and CFS area under concrete neutral axis increase the ultimate load by 14.4% and 5.3% for (BFF1 & CTF1) and (BFH1 & CTH1) respectively as shown in Fig. 11a, c. But, decreased by 9.74% for face to face (BFF2 & CTF2) position as shown in Fig. 11b.

5.6 Effect of Perforated CFS

Perforated shape of CFS were used as a new technique of encased composite beam. This type of sections increase the shear bond and reduce the section splitting compared with the flat one. Group C specimens compared with its corresponding specimens from group D. As shown in Fig. 12a, b, perforated sections increase the ultimate load by 14.75% and 29.92% for both BTB and FTF positions.

6 Conclusions

This paper presents an experimental study on the flexural performance of eleven composite concrete beams with cold formed steel section, prepared and tested to investigate the effect of changing the cold formed steel section inside the compression area, cold formed steel section arrangement inside the concrete beam, using perforated steel as an alternative technique to connect the stirrups, concrete, and cold formed steel section to improve the composite beam behavior. Based on the previous experimental results, the major conclusions are summarized as follows:

1. In all tests, section failure at the end of loading was found to be critical under combined bending. Shear splitting, and lateral torsional buckling were the failure modes observed in the specimens. For perforated cold formed steel sections, bending failure was apparent at distance equal third of the beam length from the end support, and prevented the lateral torsional buckling for the cold formed steel section.
2. For full depth CFS:
   a. Enhance the control beam ultimate load by 96.72%, 75.41% and 113.11% than the control beam without cold formed section for back to back CFS, front to front CFS, and back to back CFS with half top flange width respectively.
   b. Back to back increase ultimate load by 12.15% of that obtained for the face to face position. This

Fig. 7 Modes of failure for specimens

increasing percentage are reached to 40.76% for half depth CFS.

3. For half depth increase the control beam ultimate load by 125%, 59.85% and 125.14% for back to back CFS, front to front CFS, and back to back CFS with half top flange width respectively.
4. New shape of the perforated steel cold formed sections indicates a good enhancement of the control beam ultimate load:
   a. The ultimate load of composite beam with perforated CFS increased by 158.19% and 107.65% for back to back perforated CFS, and front to front perforated CFS respectively compared with ultimate load of the control beam.
   b. Back to back position increase the ultimate load by 24.43% than face to face position.
   c. For back to back position and CFS area under concrete neutral axis increase the ultimate load by 14.4% full depth than half depth, and 5.3% for full depth than half depth with half flange width respectively.
5. Composite beam with single horizontal perforated CFS figure out a considerable raising of the control beam

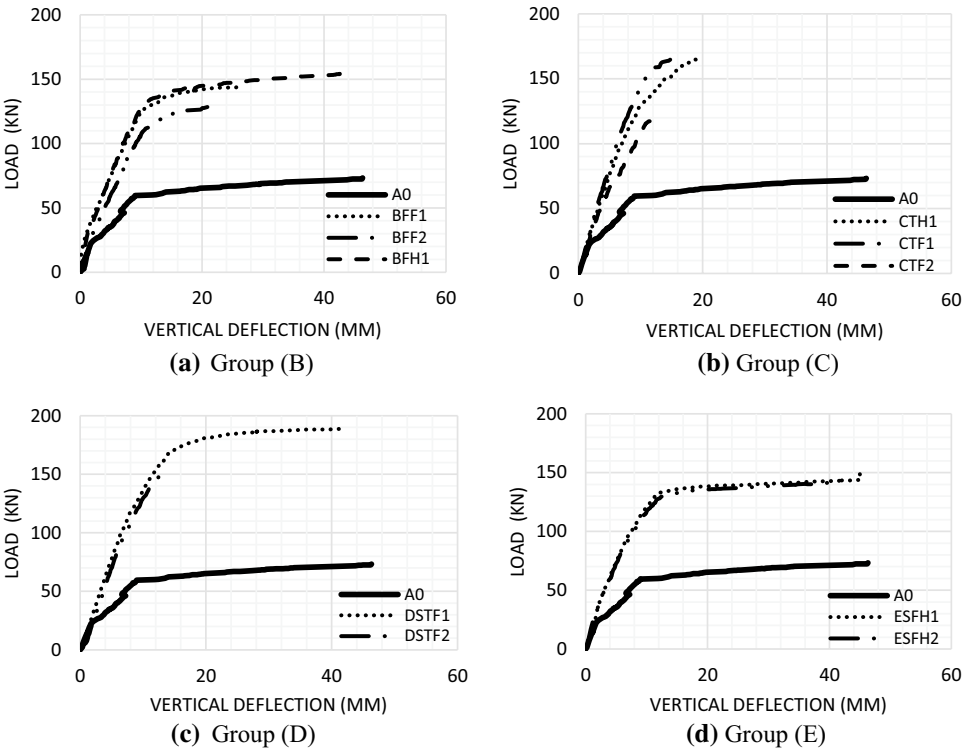

(a) Group (B) **(b)** Group (C)

(c) Group (D) **(d)** Group (E)

Fig. 8 Loads and vertical deflections relationship of the tested specimens

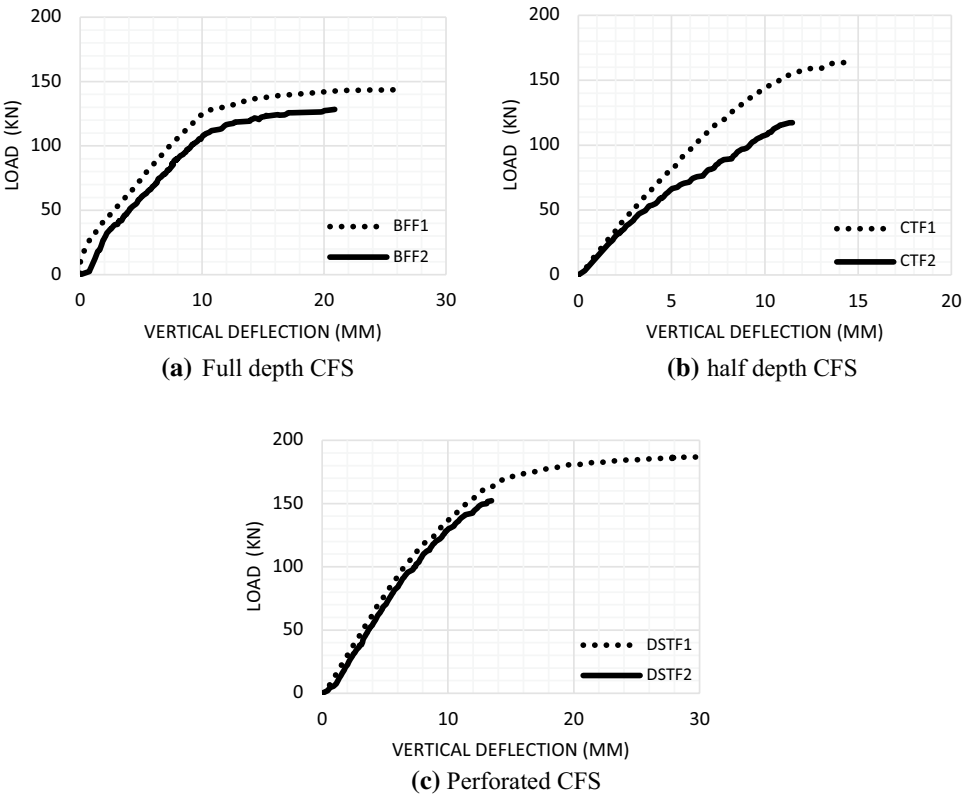

(a) Full depth CFS **(b)** half depth CFS

(c) Perforated CFS

Fig. 9 Effect of steel cold formed sections positions

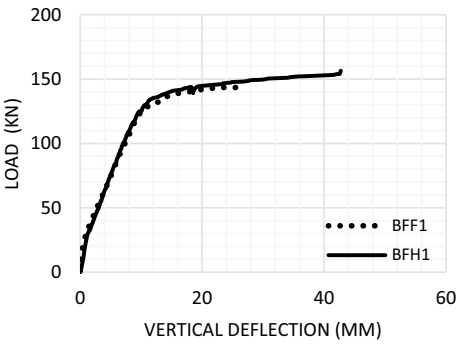

(a) Full depth CFS

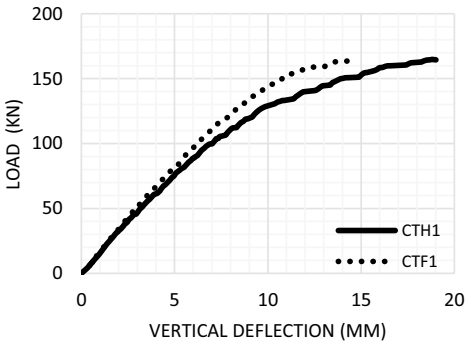

(b) half depth CFS

Fig. 10 Effect of reducing top flange of steel cold formed section

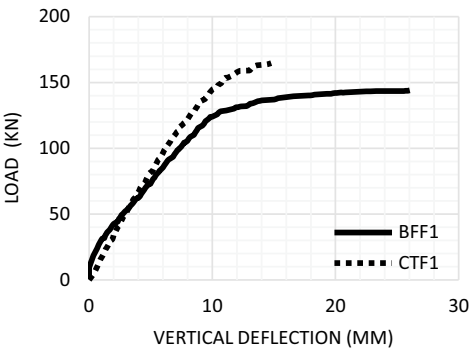

(a) Back to Back CFS

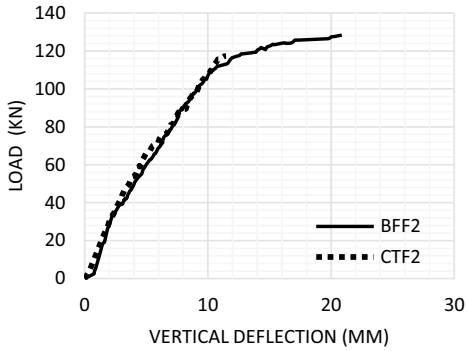

(b) Front to Front CFS

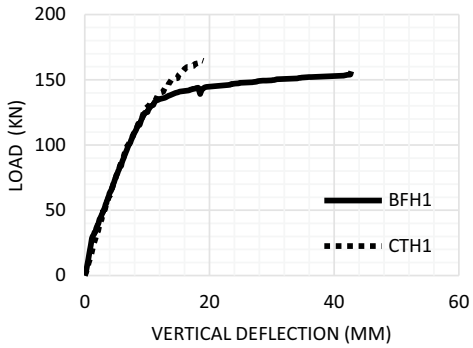

(c) Back to Back& Half flange width CFS

Fig. 11 Effect of the steel cold formed section depth

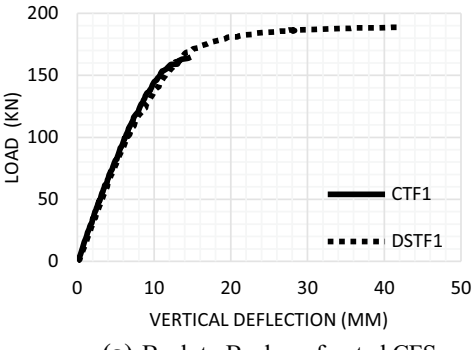

(a) Back to Back perforated CFS

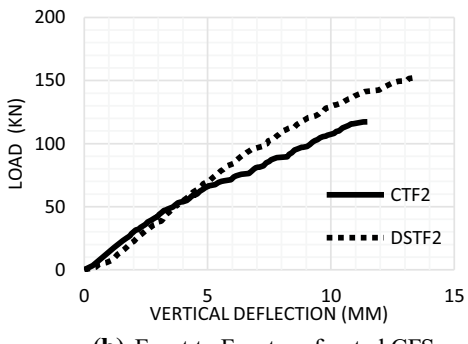

(b) Front to Front perforated CFS

Fig. 12 Effect of using flat and perforated steel cold formed section

ultimate load by 103.55% and 103.41% for upper web perforated CFS, and lower web perforated CFS respectively.

6. Reducing top flange width led to increase the ultimate load by 8.7% and 0.1% for full and half depth CFS respectively.
7. Perforated CFS sections increase the ultimate load by 14.75% and 29.92% for both BTB and FTF positions than flat CFS sections in the same positions inside the concrete beam.

References

Alhajri, T. M., Tahir, M. M., Azimi, M., Mirza, J., Lawan, M. M., Alenezi, K. K., & Ragaee, M. B. (2016). Behavior of pre-cast U-shaped composite beam integrating cold-formed steel with ferro-cement slab. *Thin-Walled Structures, 102*, 18–29.

Bamaga, S. O., Tahir, M. M., Tan, T. C., Mohammad, S., Yahya, N., Saleh, A. L., & Rahman, A. B. A. (2013). Feasibility of developing composite action between concrete and cold-formed steel beam. *Journal of Central South University, 20*(12), 3689–3696.

Dinis, P. B., & Camotim, D. (2010). Local/distortional mode interaction in cold-formed steel lipped channel beams. *Thin-Walled Structures, 48*(10–11), 771–785.

Faridmehr, I., Osman, M. H., Tahir, M. M., Azimi, M., & Gholami, M. (2016). Behaviour and design of cold-formed steel C-sections with cover plates under bending. *International Journal of Steel Structures, 16*(2), 587–600.

Foraboschi, P. (2016). Structural layout that takes full advantage of the capabilities and opportunities afforded by two-way RC floors, coupled with the selection of the best technique, to avoid serviceability failures. *Engineering Failure Analysis, 70*, 387–418.

Foraboschi, P. (2019). Lateral load-carrying capacity of steel columns with fixed-roller end supports. *Journal of Building Engineering, 26*, 100879.

Foraboschi, P. (2020). Predictive formulation for the ultimate combinations of axial force and bending moment attainable by steel members. *International Journal of Steel Structures, 20*, 1–20.

Hsu, C. T. T., Punurai, S., Punurai, W., & Majdi, Y. (2014). New composite beams having cold-formed steel joists and concrete slab. *Engineering Structures, 71*, 187–200.

Kvočák, V., Dubecký, D., & Spišák, M. (2013). The composite section analysis of encased beams with closed shape. Вісник Національного університету Львівська політехніка. *Теорія і Практика Будівництва, 756*, 135–139.

Lee, J., Kim, S. M., Park, H. S., & Woo, B. H. (2005). Optimum design of cold-formed steel channel beams using micro Genetic Algorithm. *Engineering Structures, 27*(1), 17–24.

Leng, J., Li, Z., Guest, J. K., & Schafer, B. W. (2014). Shape optimization of cold-formed steel columns with fabrication and geometric end-use constraints. *Thin-Walled Structures, 85*, 271–290.

Ma, W., Becque, J., Hajirasouliha, I., & Ye, J. (2015). Cross-sectional optimization of cold-formed steel channels to Eurocode 3. *Engineering Structures, 101*, 641–651.

Tahir, M. M., Lawan, M. M., Saggaff, A., & Mirza, J. (2016). Influence of shear connector size on ultimate strength in composite construction with cold-formed steel channel lipped section. *Review of Industrial Engineering Letters, 3*(1), 1–10.

Ye, J., Hajirasouliha, I., & Becque, J. (2018). Experimental investigation of local-flexural interactive buckling of cold-formed steel channel columns. *Thin-Walled Structures, 125*, 245–258.

Valsa Ipe, T., Sharada Bai, H., Manjula Vani, K., & Iqba, M. M. Z. (2013). Flexural behavior of cold-formed steel concrete composite beams. *Steel & Composite Structures, an International Journal, 14*(2), 105–120.

Wehbe, N., Bahmani, P., & Wehbe, A. (2013). Behavior of concrete/cold formed steel composite beams: Experimental development of a novel structural system. *International Journal of Concrete Structures and Materials, 7*(1), 51–59.

Youssef Kamal, A., & Nabih Khalil, N. (2017). Cold-formed steel u-section encased in simple support reinforced concrete beam. *Ijrdo Journal of Mechanical and Civil Engineering, 3*(10), 2456–1479.